Available online at www.sciencedirect.com
SCIENCE DIRECT®
Applied Geochemistry 21 (2006) 887–903
Applied Geochemistry
www.elsevier.com/locate/apgeochem

Geochemistry of surface and ground water in Guiyang, China: Water/rock interaction and pollution in a karst hydrological system

Yun-Chao Lang [a,b], Cong-Qiang Liu [a,*], Zhi-Qi Zhao [a], Si-Liang Li [a,b], Gui-Lin Han [a]

[a] *The State Key Laboratory of Environmental Geochemistry, Institute of Geochemistry, Chinese Academy of Sciences, Guiyang 550002, PR China*
[b] *Graduate School of Chinese Academy of Sciences, Beijing 100039, PR China*

Received 11 November 2004; accepted 14 March 2006
Editorial handling by A. Herczeg
Available online 19 May 2006

Abstract

The chemical compositions of the surface/ground water of Guiyang, the capital city of Guizhou Province, China are dominated by Ca^{2+}, Mg^{2+}, HCO_3^- and SO_4^{2-}, which have been derived largely from chemical weathering of carbonate rocks (limestone and dolomite). The production of SO_4^{2-} has multiple origins, mainly from dissolution of sulfate evaporites, oxidation of sulfide minerals and organic S in the strata, and anthropogenic sources. Most ground water is exposed to soil CO_2 and, therefore, the H_2CO_3 which attacks minerals contains much soil C. In addition, the H_2SO_4 produced as a result of the oxidation of sulfides in S-rich coal seams and/or organic S, is believed to be associated with the chemical weathering of rocks. The major anthropogenic components in the surface and ground water include K^+, Na^+, Cl^-, SO_4^{2-} and NO_3^-, with Cl^- and NO_3^- being the main contributors to ground water pollution in Guiyang and its adjacent areas. The seasonal variations in concentrations of anthropogenic components demonstrate that the karst ground water system is liable to pollution by human activities. The higher content of NO_3^- in ground water compared to surface water during the summer and winter seasons, indicates that the karstic ground water system is not capable of denitrification and therefore does not easily recover once contaminated with nitrates.

1. Introduction

Karst aquifers are those that contain dissolution-generated conduits that permit the rapid transport of ground water, often in turbulent flow, and are susceptible to rapid introduction of contaminants since the conduit system receives localized inputs from surface streams. The understanding of properties, characterization, and the evolution of karstic carbonate aquifers have improved substantially, however the hydrology of karstic aquifers is often

* Corresponding author.
E-mail address: Liucongqiang@vip.skleg.cn (C.-Q. Liu).

0883-2927/$ - see front matter © 2006 Published by Elsevier Ltd.
doi:10.1016/j.apgeochem.2006.03.005

difficult to evaluate by numerical analysis due to gross heterogeneity in permeability and hydraulic conductivity, mixed conduit and diffuse flow, variable location, and the amount of recharge and discharge (White, 2002; Scanlon et al., 2003). Extensive research has been conducted on the karstic hydrological system, which has focused on ground water flow and residence time inside the aquifer, the interactions of all components and their effects on water chemistry, and the contaminant transport processes and mechanisms in karst aquifers (Wicks and Engeln, 1997; Vaute et al., 1997; Andreo and Carrasco, 1999; Lee and Krothe, 2001; Gonfiantini and Zuppi, 2003; Plummer et al., 1998; Marfia et al., 2004).

Guizhou Province is located in SW China and is the center of the East Asian karst zone. Within the boundary of Guizhou Province, carbonate rocks are widely distributed, with their exposure covering more than 70% of the entire province. Karstification is well developed and there are many diverse karst types. Within the last 10a, the rapid development of urbanization and industrialization in addition to the over exploitation and utilization of ground water have resulted in lowering ground level, surface collapse and ground water contamination (Han and Jin, 1996). Due to the peculiar geographical and hydrogeological circumstances of karst regions, ground water is vulnerable to pollution from human activities, and once contaminated its rehabilitation is a hard and time-consuming project. Therefore systematic studies on chemical characteristics of ground waters, their movement in aquifers, water/rock interactions, and the interaction of ground and surface water are of great importance for understanding the hydrogeochemical processes, and the protection and sustainable utilization of ground water resources. The purpose of this study is to:

- Characterize water/rock interaction and its effects on the chemistry of a karstic ground water system, by studying chemical and isotopic compositions of surface/ground water.
- Understand the interaction of surface/ground water, transport, transformation and provenances of contaminants, and the influence of human activities on the hydrogeochemical environment of ground water in a karst system.
- Provide a scientific basis for protection and rational utilization of surface/ground water resources in karst regions.

2. Geography and hydrogeological background of Guiyang

Guiyang, the capital city of Guizhou Province, is located in the central part of The Province, covering an area from 26°11′00″ to 26°54′20″N and 106°27′20″ to 107°03′00″E, with elevations ranging from 875 to 1655 m above mean sea level. Guiyang has a population of more than 1.5 million people, a high diversity of karstic landforms, a high elevation and low latitude, with a subtropical warm–moist climate, annual average temperature of 15.3 °C and annual precipitation of 1200 mm.

Most of the city of Guiyang is associated with the Wujiang river catchment, one of the biggest tributaries in the upper reaches of the Changjiang River. The Nanming River is the major river flowing through the city of Guiyang from the SW via the Xiaoche River and other streams, which have an annual average discharge of 12.3 m^3/s. The Nanming River flows into the Qingshui River, one of the tributaries of the Wujiang River. Within the region studied there are two large water reservoirs, i.e., the Aha and the Huaxi Reservoirs, which are the main water supply resources for Guiyang city (Fig. 1). As shown in the hydrogeological map of Guiyang (Fig. 1a), the outcrops are principally sedimentary rocks, with Triassic strata being widespread (accounting for nearly 50% of the area), followed by the Permian strata (accounting for nearly 20%). The rock types are predominantly shallow-sea platform carbonate rocks (dolomite and limestone), with a few Late Triassic continental-facies clastic rocks. The strata within the region studied are characterized by obvious folding and well developed faults. The main aquifers in the region of Guiyang are carbonate rocks (limestone and dolomite, accounting for more than 80% of the aquifers). Other aquifers are mainly clastic rocks, some of which are interbedded with S-rich coal seams. Sulfate evaporite strata, though minor, also exist in the region studied.

The city of Guiyang is located in a basin, a catchment for surface and ground water. Both surface and ground water flow mainly from north and south to the center of the basin (Fig. 1b). Several factories of various sizes are located on both banks of the Nanming River. Since the downtown portion of Guiyang is located in the center of the basin, ground water within the region studied is subjected to the influence of human activities. Municipal sewage

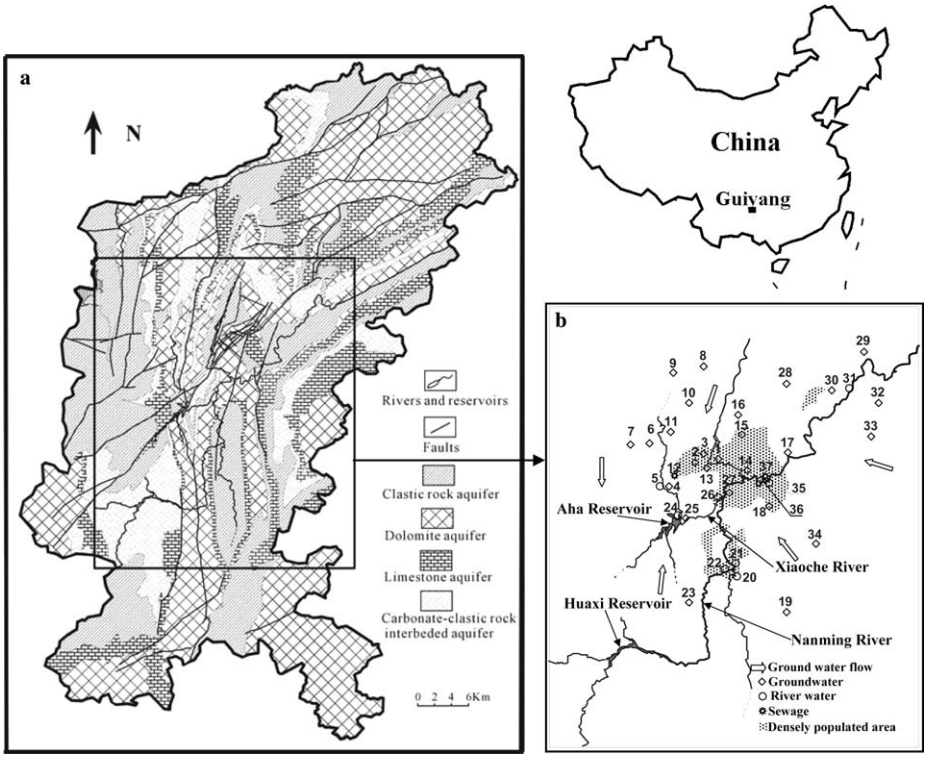

Fig. 1. Hydrogeological map of Guiyang, SW China, and its surroundings, showing the lithology and structure of the studied area (a), sampling locations and sample numbers (b). Modified from (Han and Jin, 1996).

discharged from enterprises, factories and households on both sides of the Nanming River gives rise to complicated sources of pollutants in surface/ground water. The Aha Reservoir as one of the important water supply sources is often reported to contain elevated amounts of Fe, Mn and SO_4^{2-}, mainly due to coal mining in the upper reaches.

3. Samples and analytical procedure

3.1. Sample description

Surface (river and lake) and ground water samples were collected from downtown Guiyang and its surroundings (Fig. 1b) over two seasons: 37 water samples were collected in January 2002 (winter), and another 35 water samples were collected in August of the same year (summer). At the two sampling sites, 37 and 12, four municipal sewage samples were collected during winter and summer; sampling site 37 is the outlet of municipal sewage close to the Naming River, and sampling site 12 is near to the Guiyang Tyre Plant. The ground water samples were collected from wells (bore holes) and various types of springs (Table 1). Of the ground water samples, spring and well samples collected at sites 1, 2, 4, 7, 11, 13, 14, 27, 33 and 36 are confined aquifer waters. The rest of the samples are mainly gravity spring (unconfined) water. Sample No. 15 had a strong odour of gasoline because of contamination caused by a gasoline leak event near a Petrol Station. Sample No. 7 was spring water, which was influenced by coal-containing strata. A large amount of brownish deposits (Fe and Mn oxides) were found along the spring outlet and the channel. Two river water samples were collected at site 5, polluted due to the input of coal mining water in the upper reaches.

3.2. Analytical procedure

Water temperature (T), pH and electrical conductivity (EC) were measured on site. The water samples were collected in polyethylene bags that had been cleaned with acid. All acid reagents were ultra-purified by sub-boiling distillation methods. Millipore ultra-pure water was used in the

Table 1
Groundwater samples collected in Guiyang city, SW China

Sampling sites (sample names)	Description	Discharge L/s	Aquifer
1 (GYK-1,GYF-1)	Well (depth, 396 m)	15.3	Dolomite
2 (GYK-2,GYF-2)	Well (depth, 236 m)	16.7	Lime stone + gypsum layer + dolomite
3 (GYK-3,GYF-3)	Gravity spring	35	Dolomite
4 (GYK-4,GYF-4)	Gravity spring	3	Dolomite, with minor limestone
6 (GYK-6)	Gravity spring	41.2	Dolomite, with quaternary deposit cover
7 (GYK-7)	Artesian spring	5	Shale, coal-containing + minor limestone
8 (GYK-8,GYF-8)	Artesian spring	5	Limestone + minor shale layers
9 (GYK-9,GYF-9)	Gravity spring	32.5	Dolomite + limestone
10 (GYK-10,GYF-10)	Gravity spring	58.7	Dolomite
11 (GYK-11,GYF-11)	Well (depth, 250 m)	5.6	Dolomite
13 (GYK-13,GYF-13)	Well (depth, 209 m)	3.3	Dolomite
14 (GYK-14,GYF-14)	Well (depth, 300 m)	6	Dolomite + limestone
15 (GYK-15,GYF-15)	Gravity spring	No data	Limestone
16 (GYK-16,GYF-16)	Gravity spring	1	Dolomite + minor clastic rock
17 (GYK-17,GYF-17)	Gravity spring	5	Limestone + dolomite
18 (GYK-18,GYF-18)	Gravity spring		Dolomite + limestone
19 (GYK-19,GYF-19)	Gravity spring	4.4	Limestone
23 (GYK-23,GYF-23)	Gravity spring	3.3	Dolomite
25 (GYK-25,GYF-25)	Gravity spring	No data	Limestone
27 (GYK-27,GYF-27)	Well (depth, 275 m)	8	Limestone + dolomite
28 (GYK-28,GYF-28)	Gravity spring	0.1	Dolomite + limestone
29 (GYK-29,GYF-29)	Artesian spring	74.1	Limestone + shale
30 (GYK-30,GYF-30)	Gravity spring	0.05	Dolomite + quaternary deposits
32 (GYK-32,GYF-32)	Gravity spring	0.01	Clastic rocks + minor limestone
33 (GYK-33,GYF-33)	Artesian spring	1571	Limestone + dolomite
34 (GYK-34,GYF-34)	Gravity spring	15.4	Limestone + dolomite
36 (GYK-36,GYF-36)	Well (depth, 350 m)	6.3	Limestone

Note. GYK- stands for winter sample, while GYF- for summer sample; the discharge data (L/s) were observed in 1990 (data from hydrological report issued by Bureau of Geology and Mining of Guizhou Province); the ground water at sites 6 and 7 could not be sampled in summer.

experiment (the electrical resistance is 18.2 MΩ/cm), and all chemical analyses of the samples were performed by the State Key Laboratory of Environment Geochemistry, Institute of Geochemistry, Chinese Academy of Sciences.

HCO_3^- was determined using the HCl titration method within hours of sample collection. All of the samples were filtered through 0.45 μm acetate rayon filtering membrane prior to analysis for anions and cations. The cations (K^+, Na^+, Ca^{2+}, Mg^{2+}) were determined by atomic absorption spectrometry (AAS), while the anions (F^-, Cl^-, $NO_2^-, NO_3^-, SO_4^{2-}$) were determined by high-efficiency liquid chromatography.

To separate Sr from major elements in the water samples for measurement of Sr isotopic composition, the filtered water samples were directly passed through an AG50W-50 resin column in a 2 N HCl medium. The isotopic compositions of Sr were determined by MC-ICP-MS (multi collector-inductively coupled plasma-mass spectrometer, produced by Nu Instrument Ltd., UK), for the samples collected in the summer, at the Institute of Geochemistry, Chinese Academy of Sciences, Guiyang, and on a VG-354 mass spectrometer, for the samples collected in the winter, at the Institute of Geology and Geophysics, Beijing. The value $^{87}Sr/^{86}Sr$ for the NBS987 strontium standard, measured on the VG-354, was 0.710275 ± 0.000021 (2σ, $n = 12$), and measured on the MC-ICP-MS, was 0.710278 ± 0.000018 (2σ, $n = 66$) during the measurement period of the samples. For quality control of the MC-ICP-MS measurement, the NBS987 standard was generally measured two to three times for every three samples. Although the samples collected during winter and summer were measured on different mass spectrometers, comparative analyses for 10 samples performed on both the VG354 and MC-ICP-MS, showed no significant difference between the two data sets. The procedure for determination of $\delta^{13}C$ in dissolved inorganic C (DIC) in surface and ground water samples, is described in Li et al. (2005).

4. Results

4.1. Seasonal variation in ground and surface water

The chemical compositions of ground water, river water and sewage samples collected in the winter and summer seasons are listed in Table 2. Ground water in the karst regions is usually alkaline. With the exception of sample No. 7, the pH values of all ground water samples collected in winter are within the range of 6.7–8.0 (averaging 7.3, $T = 16.2$ °C), while those of ground water samples collected in summer vary over a smaller range from 6.9 to 7.8 (averaging 7.4, $T = 18.3$ °C). Surface water pH values ranged from 7.1 to 8.1 in winter and 7.8 to 8.3 in summer.

The average TDS values were 614 and 564 mg/L for ground water in winter and summer, respectively, showing that the TDS values of ground water in winter are higher. Similarly, the surface water samples collected in winter have higher TDS contents (average value, 548 mg/L), as compared to those collected in summer (average value, 403 mg/L). Especially in summer, the ground water generally has higher TDS values than the surface water. For most of the chemical components analyzed, both ground and surface water show higher concentration in winter than in summer. Chloride and Na^+ show significantly higher concentrations in the winter samples compared to the summer samples. In summer, all of the components, except for pH and K, show significantly higher concentrations in the ground water than in the surface water. In winter, however, TDS, Ca^{2+}, Cl^- and SO_4^{2-} concentrations are almost the same, K^+ and Na^+ are lower, and Mg^{2+}, NO_3^- and SiO_2 are higher in the ground water than in the surface water. Nitrate concentrations in the ground water samples, on average, are higher in summer than in winter, but are almost the same for the surface water in both seasons. Compared with the surface water, ground water shows markedly higher NO_3^- concentrations in both seasons. Silica in ground water shows higher concentrations than in the surface water in both seasons, and is greatly enriched in winter ground water.

4.2. Variation in chemical composition

Variations in chemical composition of the ground and surface waters are shown in Fig. 2. As seen from the triangular diagrams for anions and cations, ground waters are dominated by Ca^{2+}, Mg^{2+}, HCO_3^- and SO_4^{2-}, which account for more than 80% of total cations and anions. Of the cations, Ca^{2+} is the most dominant and accounts for more than 50%, while Na^+ and K^+ are generally lower than 20%. The HCO_3^- and SO_4^{2-} anions are dominant with Cl^- and NO_3^- accounting for less than 20% of the anions for most of the water samples. Sample locality No. 3 is in a factory in Guiyang, the water collected there has high concentrations of $K^+ + Na^+$, and $Cl^- + NO_3^-$. Compared to ground and surface water samples, the two sewage samples collected in both summer and winter show higher K^+, Na^+, Cl^- and SO_4^{2-}, but lower NO_3^-.

4.3. Strontium and Sr isotopes

Strontium concentrations and the $^{87}Sr/^{86}Sr$ ratios of the water samples are listed in Table 3. The Sr concentrations of the ground waters are very variable, ranging from 1.14 to 184 μmol/L. The ground water samples, GYK-2 and GYF-2, collected from a gypsum-rich aquifer have the highest Sr concentrations in both summer and winter. Most of the ground water samples have Sr concentrations in the range 2–5 μmol/L. The surface water samples have Sr concentrations from 4.65 to 15.1 μmol/L in winter and from 1.83 to 6.85 μmol/L in summer; winter river water samples in general have higher Sr concentrations than summer river water samples.

The ground water in winter has Sr isotopic ratios varying from 0.70734 to 0.71081, slightly lower than those of the ground water in summer (0.70756–0.71175). The river water has relatively constant Sr isotopic compositions, with $^{87}Sr/^{86}Sr$ ratios varying from 0.70760 to 0.70814 in winter and from 0.70770 to 0.70891 in summer. The Sr isotopic ratios of the two sewage samples in both winter and summer are constant, around 0.70800.

4.4. Isotopic composition of DIC

Although the isotope ratios of DIC have previously been used to discuss C cycling in the surface/ground water systems (Li et al., 2005), they are reproduced here (Table 3), so that they can be used along with the Sr isotope ratios and chemical data in the present study. The $\delta^{13}C$ values of DIC in ground water range from −12.8‰ to −7.8‰ in winter and from −14.4‰ to −8.5‰ in summer; in winter ground water DIC contains more ^{13}C than that of ground water in summer. The ground water

Table 2
Temperature, pH values and concentration data of major ions in surface, ground and sewage water samples collected from Guiyang City, SW China

No.	T (°C)	pH	K^+ (mmol/L)	Na^+ (mmol/L)	Ca^{2+} (mmol/L)	Mg^{2+} (mmol/L)	F^- (mmol/L)	NO_3^- (mmol/L)	Cl^- (mmol/L)	SO_4^{2-} (mmol/L)	HCO_3^- (mmol/L)	SiO_2 (mmol/L)	TDS (mg/L)
Winter ground waters													
GYK-1	21.0	7.53	0.06	0.22	1.18	1.07	nd	nd	0.09	0.11	4.43	0.15	364.31
GYK-2	17.1	6.91	0.10	2.52	9.92	1.88	0.06	nd	0.30	11.17	4.49	0.23	1813.50
GYK-3	15.0	7.68	0.23	1.52	1.85	1.30	0.01	0.15	3.25	1.09	4.08	0.07	651.03
GYK-4	17.0	6.57	0.24	1.24	2.48	1.25	nd	0.32	1.01	2.71	3.15	0.11	674.99
GYK-6	19.1	7.56	0.01	0.08	1.44	1.10	nd	0.14	0.19	0.23	4.15	0.08	377.12
GYK-7	15.0	5.96	0.35	1.45	4.66	1.72	nd	nd	0.41	8.41	3.23	0.13	1294.16
GYK-8	14.2	6.93	0.04	0.29	2.00	0.78	nd	0.45	0.17	0.49	3.37	0.06	393.55
GYK-9	14.2	6.62	0.15	1.03	1.70	0.97	0.03	nd	0.89	1.11	3.79	0.16	490.02
GYK-10	14.5	7.86	0.02	0.23	1.60	1.12	0.02	0.40	0.20	0.28	4.32	0.07	419.35
GYK-11	15.0	6.79	0.05	0.29	1.82	1.32	0.03	0.14	0.40	0.46	4.96	0.09	482.44
GYK-13	16.0	7.12	0.14	0.23	1.02	0.84	0.04	nd	0.12	0.47	2.75	0.20	288.36
GYK-14	16.7	6.79	0.26	1.14	3.59	0.98	nd	0.55	1.07	1.92	5.15	0.24	773.96
GYK-15	16.1	6.83	0.17	1.01	3.32	0.55	0.02	0.27	3.91	1.24	3.84	0.18	685.24
GYK-16	14.8	7.26	0.09	0.44	2.27	1.32	0.03	0.35	0.37	1.68	3.96	0.07	573.52
GYK-17	16.1	7.52	0.22	0.85	3.71	0.45	nd	0.48	1.08	1.36	4.98	0.23	689.92
GYK-18	16.0	7.58	0.07	0.74	2.47	1.29	nd	0.26	0.72	1.44	5.11	0.09	641.34
GYK-19	16.1	7.55	0.01	0.09	2.22	0.61	nd	0.14	0.25	0.19	4.32	0.17	405.05
GYK-23	15.8	7.70	0.01	0.09	2.09	1.26	0.01	0.08	0.15	0.51	5.03	0.05	482.68
GYK-25	17.3	7.64	0.02	0.02	2.70	0.18	nd	0.09	0.07	0.83	4.17	0.18	456.67
GYK-27	15.5	7.55	0.08	0.92	2.72	1.52	nd	0.12	1.19	2.50	4.20	0.05	715.60
GYK-28	17.1	7.59	0.03	0.06	2.03	1.36	nd	0.13	0.51	0.17	5.44	0.06	489.84
GYK-29	16.0	7.71	0.04	0.15	2.43	0.69	nd	0.06	0.72	0.76	3.92	0.09	460.23
GYK-30	16.0	8.01	0.21	1.24	2.46	1.08	nd	nd	1.14	0.97	6.52	0.45	692.14
GYK-32	17.0	7.54	0.04	0.06	2.14	0.10	nd	0.15	0.71	0.08	3.37	0.21	339.27
GYK-33	15.0	7.96	0.04	0.14	2.10	0.39	nd	0.09	0.13	0.38	3.82	0.01	378.54
GYK-34	17.0	7.33	0.03	0.29	2.76	0.86	nd	0.27	0.29	0.66	4.97	0.12	532.07
GYK-36	18.0	6.86	0.09	0.73	3.23	1.48	nd	0.63	0.94	1.57	5.40	0.06	737.46
Summer ground waters													
GYF-1	22.2	7.5	0.06	0.20	1.09	1.04	nd	nd	0.01	0.11	4.85	0.13	382.21
GYF-2	17.7	7.03	0.08	0.37	9.75	2.80	nd	nd	0.55	10.79	4.87	0.20	1821.60
GYF-3	18.4	7.8	0.07	0.26	1.76	0.83	0.03	0.25	0.16	0.78	3.80	0.08	426.89
GYF-4	18.4	7.18	0.19	0.72	3.10	1.33	nd	0.84	0.59	2.33	3.83	0.10	710.14
GYF-6	No	No	No	No	No	No	No	No	No	No	No	No	No
GYF-7	No	No	No	No	No	No	No	No	No	No	No	No	No
GYF-8	16.4	7.39	0.02	0.70	1.81	0.36	0.2	0.17	0.07	0.39	4.44	0.07	419.67
GYF-9	18.3	7.48	0.11	0.44	1.65	0.75	0.05	0.16	0.26	0.93	3.65	0.07	429.29
GYF-10	18.3	7.75	0.03	0.19	1.61	1.02	0.01	0.43	0.13	0.46	4.35	0.07	435.61

GYF-11	18.6	7.59	0.12	0.35	1.72	0.85	0.03	0.20	0.26	0.59	4.38	0.08	446.95
GYF-13	17.3	7.78	0.16	0.16	1.40	0.97	nd	nd	0.08	0.94	3.26	0.13	381.21
GYF-14	18.2	7.09	0.27	0.94	3.37	1.08	nd	0.60	0.94	1.94	5.63	0.16	792.73
GYF-15	17.7	7.18	0.17	0.79	3.40	0.62	nd	0.76	0.79	1.91	4.50	0.12	708.57
GYF-16	16.9	7.5	0.14	0.30	2.86	1.29	nd	0.23	0.22	1.85	4.02	0.09	602.74
GYF-17	18.2	7.07	0.11	0.53	2.75	0.32	nd	0.84	0.73	1.04	3.94	0.10	551.80
GYF-18	17.3	7.25	0.07	0.54	2.60	1.58	nd	0.33	0.52	1.72	5.08	0.07	671.02
GYF-19	16.8	7.29	0.02	0.10	2.33	0.38	nd	0.14	0.15	0.28	4.57	0.11	424.81
GYF-23	16.8	7.37	0.01	0.08	1.70	1.35	nd	0.13	0.11	0.64	5.29	0.06	498.37
GYF-25	18.7	7.37	0.02	0.03	2.51	0.18	nd	0.02	0.03	0.94	3.55	0.11	415.62
GYF-27	17.9	7.19	0.07	0.89	3.00	2.10	nd	0.80	1.18	2.28	4.88	0.06	802.46
GYF-28	17.7	7.18	0.11	0.18	1.67	1.48	nd	0.36	0.16	0.43	5.76	0.08	531.72
GYF-29	17.7	7.59	0.02	0.04	1.79	0.43	nd	0.08	0.03	0.54	3.83	0.08	374.72
GYF-30	20.6	7.39	0.18	0.33	1.26	0.60	nd	0.18	0.28	0.62	3.32	0.09	362.50
GYF-32	20.5	7.33	0.06	0.14	1.07	0.14	nd	0.53	0.12	0.33	1.91	0.10	236.95
GYF-33	18.7	6.92	0.03	0.07	1.24	0.21	nd	0.13	0.06	0.32	3.16	0.08	290.89
GYF-34	18.9	7.32	0.04	0.14	2.01	0.91	nd	0.32	0.10	1.21	3.79	0.07	477.50
GYF-36	19.5	7.34	0.11	0.64	2.82	1.68	nd	0.62	0.89	1.60	4.52	0.10	671.91
Winter surface waters													
GYK-5	12.0	7.66	0.22	1.41	2.22	1.25	0.07	0.19	0.92	2.65	3.07	0.02	645.86
GYK-20	7.8	8.02	0.15	0.78	1.65	0.64	0.02	0.04	0.56	0.76	3.64	0.06	422.75
GYK-21	9.3	8.07	0.11	0.39	1.78	0.71	0.01	0.16	0.37	0.69	3.34	0.01	394.31
GYK-22	9.6	7.86	0.10	0.36	1.87	0.72	0.01	0.16	0.34	0.67	3.30	0.03	391.13
GYK-24	9.2	8.06	0.10	0.34	3.03	0.79	nd	0.02	0.31	2.86	2.02	0.01	562.12
GYK-26	10.1	7.63	0.09	0.33	2.91	0.72	nd	0.52	0.57	2.61	2.11	0.01	577.24
GYK-31	10.6	7.81	0.34	2.32	3.23	0.95	nd	0.02	1.79	2.09	4.90	0.19	783.00
GYK-35	9.8	7.10	0.24	1.05	2.58	0.87	nd	0.11	1.31	1.47	3.81	0.05	583.45
Summer surface waters													
GYF-5	19.2	8.34	0.12	0.31	1.76	0.77	0.03	0.25	0.23	1.04	3.43	0.07	432.98
GYF-20	20.8	8.00	0.07	0.19	1.15	0.36	nd	0.07	0.13	0.52	2.34	0.08	263.07
GYF-21	20.8	8.08	0.09	0.23	1.54	0.50	nd	0.15	0.19	0.73	3.18	0.08	362.75
GYF-22	20.8	8.18	0.07	0.17	1.73	0.52	nd	0.22	0.15	0.74	3.68	0.08	402.72
GYF-24	22.1	8.03	0.09	0.25	2.05	0.74	0.01	0.10	0.20	2.22	1.87	0.02	449.24
GYF-26	21.0	8.15	0.09	0.27	2.28	0.72	0.01	0.15	0.21	1.93	2.69	0.05	483.99
GYF-31	21.2	7.80	0.16	0.34	1.51	0.53	0.01	0.16	0.35	1.01	2.94	0.09	386.19
GYF-35	22.1	7.77	0.11	0.32	1.97	0.65	0.01	0.14	0.30	1.49	2.33	0.07	410.36
Winter sewage													
GYK-12	30.5	6.50	0.19	1.29	2.50	0.93	0.01	nd	1.28	2.94	2.82	0.04	659.53
GYK-37	13.5	7.66	0.36	2.69	2.60	0.70	nd	nd	1.81	1.56	5.03	nd	717.31
Summer sewage													
GYF-12	26.9	7.70	0.17	1.51	2.62	0.99	nd	0.13	1.03	2.57	3.11	0.09	651.46
GYF-37	24.5	7.67	0.31	1.84	3.71	1.64	nd	nd	1.07	1.18	3.67	0.12	617.12

Note. "nd" means no data because the concentration is under detection limit; "no" means no data because the samples could not be collected in winter.

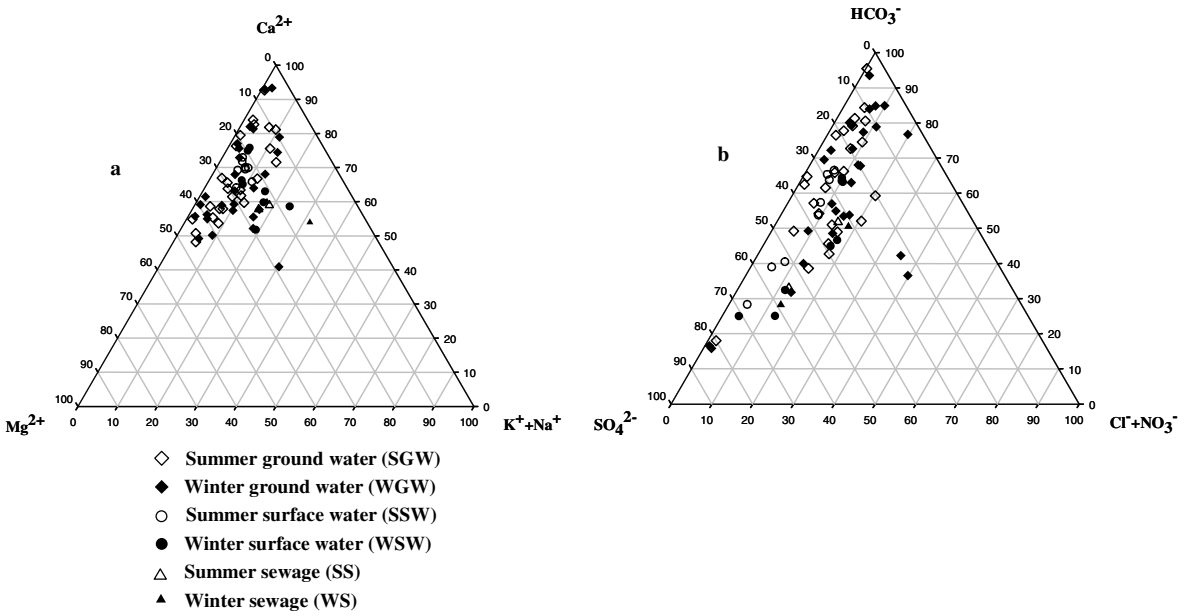

Fig. 2. Triangular diagrams showing compositional variations of the major cations (a) and anions (b) in surface and ground water.

from the aquifer containing gypsum layers shows the highest $\delta^{13}C$ value, while the ground water samples contaminated by oil leakage (GYK-15 and GFY-15) have the lowest $\delta^{13}C$ values. Compared to ground water, the surface water samples show higher $\delta^{13}C$ values, ranging from $-10.0‰$ to $-4.8‰$. With the exception of sample GYF-24, all of the surface water samples collected in winter have higher $\delta^{13}C$ values compared to those collected in summer.

5. Discussion

5.1. Surface/ground water interaction

Sinkholes, conduits and caves form large secondary pathways for subsurface flow in karstic terrain, and so, the discharge of ground water quickly responds to surface water and shows wide variations in flow rate, water chemistry and stable isotopic composition. Plummer et al. (1998) studied river water flow into a karstic limestone aquifer through tracing the young fraction in groundwater mixtures in the Upper Floridan Aquifer near Valdosta, Georgia, by using multiple geochemical tracers. Lee and Krothe (2001) identified the unique signatures of rain, soil, epikarstic and phreatic waters by using DIC and $\delta^{13}C$ as tracers, and created a four-component mixing model that describes the water, solute and solute isotopic fluxes. Their studies demonstrate the important contribution of water infiltrating through the soil layer displacing water in the vadose zone after major storm events, thus mobilizing agricultural contaminants to the major discharge points. Desmarais and Rofstaczer (2002) after studying the chemical and physical response of a spring to storm events showed that storm response is fairly consistent and repeatable, independent of the time between storms and the configuration of the rain event itself, and that spring flow is likely controlled by displaced water from the aquifer rather than by direct recharge through the soil zone.

By comparing the water chemistry of ground and surface waters in both winter and summer seasons (Fig. 3), an understanding may be gained of the interaction between surface water (and/or soil water) and ground water. In Fig. 3, ion ratios are used for comparison, since utilization of the ion ratio can negate concentration or dilution effects. In both surface and ground waters, Na^+ relative to Ca^{2+}, and Cl^- relative to HCO_3^- are enriched in winter samples compared to summer samples, while NO_3^- relative to HCO_3^- is enriched in most of the ground and surface water samples in summer. The co-variations in chemical composition of both surface and ground water suggest a quick response of the ground water system to

Table 3
Sr concentration and isotopic ratios of surface, ground waters and sewage collected from Guiyang City, SW China

Samples	Winter season (in January of 2002)			Samples	Summer season (in August of 2002)		
	Sr (μmol/L)	$^{87}Sr/^{86}Sr$	$\delta^{13}C$		Sr (μmol/L)	$^{87}Sr/^{86}Sr$	$\delta^{13}C$
Ground waters							
GYK-1	4.26	0.70904 ± 2	−8.4	GYF-1	4.22	0.70915 ± 18	−10.0
GYK-2	172.88	0.70790 ± 2	−5.1	GYF-2	184.32	0.70802 ± 1	−5.5
GYK-3	10.51	0.70812 ± 2	No data	GYF-3	3.99	0.70829 ± 2	−9.7
GYK-4	11.73	0.70797 ± 3	−10.7	GYF-4	9.47	0.70810 ± 3	−11.3
GYK-6	3.80	0.70813 ± 2	−8.4	GYF-6	No data	No data	No data
GYK-7	55.49	0.70734 ± 2	−11.4	GYF-7	No data	No data	No data
GYK-8	4.30	0.70791 ± 2	−7.8	GYF-8	3.31	0.70805 ± 3	−10.3
GYK-9	12.02	0.70808 ± 2	−9.0	GYF-9	6.39	0.70827 ± 2	−9.3
GYK-10	3.37	0.70803 ± 2	−8.3	GYF-10	2.28	No data	−10.0
GYK-11	10.49	0.70800 ± 2	−8.1	GYF-11	4.91	0.70815 ± 3	−9.0
GYK-13	20.13	0.70895 ± 2	−7.8	GYF-13	25.68	No data	−8.5
GYK-14	3.97	0.70903 ± 1	−9.8	GYF-14	4.22	0.70905 ± 2	−11.9
GYK-15	3.38	0.70801 ± 2	−12.8	GYF-15	6.28	0.70806 ± 4	−14.4
GYK-16	5.60	0.70818 ± 2	−10.4	GYF-16	7.53	0.70810 ± 4	−12.3
GYK-17	3.36	0.70791 ± 2	No data	GYF-17	2.40	0.70818 ± 7	No data
GYK-18	5.18	0.70818 ± 1	−9.0	GYF-18	4.22	0.70809 ± 2	−11.6
GYK-19	3.26	0.70804 ± 2	−9.2	GYF-19	3.65	0.70792 ± 4	−10.8
GYK-23	1.85	0.70831 ± 2	−9.7	GYF-23	1.83	0.70835 ± 3	−10.4
GYK-25	2.23	0.70757 ± 2	−8.4	GYF-25	1.94	0.70756 ± 2	−10.1
GYK-27	3.42	0.70820 ± 2	−10.1	GYF-27	3.77	0.70810 ± 4	−10.8
GYK-28	1.41	0.70825 ± 2	−9.3	GYF-28	1.60	0.70842 ± 3	−10.2
GYK-29	3.37	0.70784 ± 2	−8.7	GYF-29	1.83	0.70810 ± 2	−9.8
GYK-30	15.20	0.70805 ± 2	−11.5	GYF-30	3.31	0.70821 ± 3	−11.8
GYK-32	1.19	0.71081 ± 2	−10.2	GYF-32	1.14	0.71175 ± 3	−11.2
GYK-33	2.57	0.70768 ± 2	−8.6	GYF-33	1.83	0.70801 ± 3	−9.8
GYK-34	2.04	0.70821 ± 2	−8.8	GYF-34	2.74	0.70836 ± 2	−9.3
GYK-36	3.52	0.70829 ± 2	−10.0	GYF-36	3.88	0.70832 ± 3	−11.3
Surface waters							
GYK-5	15.06	0.70789 ± 2	−7.5	GYF-5	5.93	0.70806 ± 2	−8.7
GYK-20	4.66	0.70814 ± 2	−8.7	GYF-20	1.83	0.70891 ± 3	−9.2
GYK-21	5.55	0.70802 ± 2	−8.1	GYF-21	4.57	0.70812 ± 2	−9.6
GYK-22	4.65	0.70793 ± 2	−8.3	GYF-22	6.51	0.70796 ± 2	−9.2
GYK-24	9.25	0.70760 ± 2	−7.4	GYF-24	7.76	0.70770 ± 1	−4.8
GYK-26	8.47	0.70764 ± 2	−7.4	GYF-26	7.42	0.70780 ± 3	−7.7
GYK-31	7.10	0.70789 ± 2	−7.1	GYF-31	4.91	0.70816 ± 2	−9.9
GYK-35	7.01	0.70793 ± 2	−8.9	GYF-35	6.85	0.70809 ± 3	−10.0
Sewage							
GYK-12	10.25	0.70804 ± 2	−10.4	GYF-12	8.90	0.70800 ± 3	−10.7
GYK-37	6.28	No data	No data	GYF-37	4.91	0.70800 ± 3	No data

Note. Errors of the isotopic ratios are expressed in 2σ.

surface water. Strontium isotope ratios of almost all of the ground and surface water samples collected in summer are higher compared with those of the ground and surface water samples collected in winter, suggesting that more Sr is derived from dissolution of silicate minerals or from the soil zone in summer. Similarly, the ground and surface water in summer has lower $\delta^{13}C_{DIC}$ values, also suggesting more DIC derived from oxidation of organic materials in soil.

5.2. Anthropogenic inputs into the surface/ground water system

Nitrate is an important pollutant in the environment, being generally derived from agricultural fertilizers, atmospheric input, human and animal excreta and bio-combustion, and also from the nitrification of organic N and NH_4^+ (Savoie and Prospero, 1989; Agrawal et al., 1999; Jeong, 2001; Xiao and Liu, 2002). In a pollution-free area it is

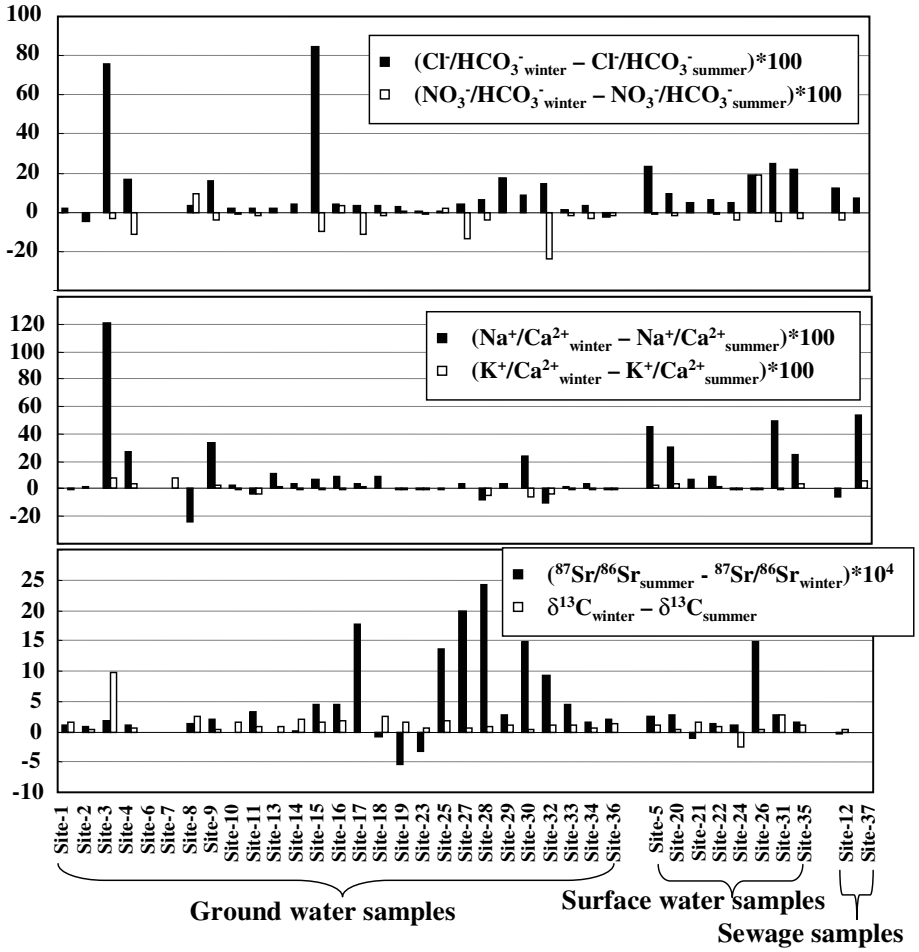

Fig. 3. Seasonal variations in chemical and isotopic compositions of ground and surface waters collected from Guiyang, SW China.

produced by soil organic matter decay through bacteria such as *Nitrosomonas* and *Nitrobacter*. Studies in Australian arid zones have shown that bacteria associated with certain soil termites can also cause considerable NO_3^- enrichment of shallow ground water under flash desert precipitation events (Barnes et al., 1992).

Compared with those collected from scarcely populated agricultural areas, ground and surface water samples collected from the metropolitan area are relatively high in NO_3^- contents. This distribution trend of NO_3^- in the ground water is more pronounced in summer (Fig. 4a); as stated earlier, ground water has significantly higher NO_3^- contents in summer than winter. Although the averages of NO_3^- contents for surface water in both summer and winter are almost the same, the HCO_3^- normalized values (NO_3^-/HCO_3^-) of surface water in summer are obviously higher than those of the winter surface water. High concentrations of NO_3^- in the sampled ground water in both winter and summer indicate that the karstic ground water system is sensitive to the influence of point and non-point pollution.

Four sewage samples collected from two locations in winter and summer show high concentrations of Cl^-, Na^+, K^+ and SO_4^{2-}, but contain almost no NO_3^-, which is presumably because $NH4^+$ and/or NO_2^- were not oxidized, or to consumption of NO_3^- by oxidation of organic materials in the sewage through the reactions below:

$$1/4CH_2O + 1/5NO_3^- + 1/5H^+ = 1/10N_2 + 1/4CO_2 + 7/20H_2O \quad (1)$$

and/or

$$4NO_3^- + 5C_{org} = 2CO_3^{2-} + 3CO_2 + 2N_2 \quad (2)$$

Denitrifying bacteria can convert NO_3^- back to N_2O and N_2 by anaerobic reduction, but in the absence of such a process, NO_3^- infiltrating deep

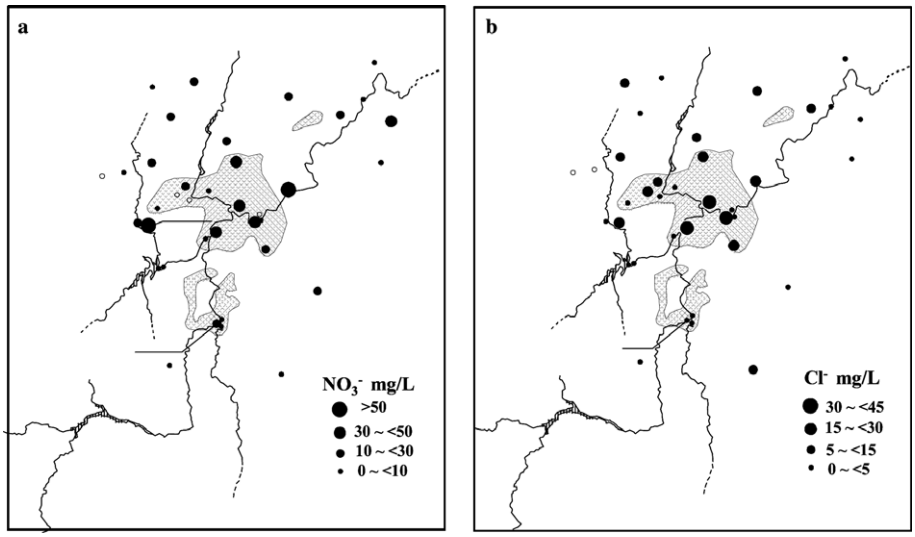

Fig. 4. Spatial variations of NO_3^- (a) and Cl^- contents (b) of the ground water in summer. Open circle = no data.

into aquifers may remain as such for a long time (Agrawal et al., 1999). The ground water samples collected in both summer and winter have higher NO_3^- concentrations and also higher NO_3^-/HCO_3^- ratios than the studied surface water samples. This suggests that the karstic ground water system does not produce conditions favorable for denitrification, and hence is not easily self-remediated once contaminated by NO_3^-.

Similar to the distribution of NO_3^- contents, the contents of Cl^- in the ground water samples collected from the central area of the city and the industrial areas, or from the sampling sites along the Nanming River are higher than those from adjacent areas, suggesting that the discharge of waste water from industrial and commercial–residential areas has led to the increase of both Cl^- and NO_3^- in ground water (Fig. 4b) in the center of the basin. Unlike NO_3^-, Cl^- is conservative or chemically inactive, so its concentrations in surface water from the upper reaches increases along the Naming River in both winter and summer, suggesting an increase of anthropogenic input to the surface water. Fig. 5 shows the relationship between HCO_3^- normalized SO_4^{2-} and Cl^- values in surface, ground water and municipal sewage samples. The municipal sewage samples contain both high Cl^- and SO_4^{2-} concentrations, and possibly have led to contamination of ground water, as seen from the general positive correlation between Cl^-/HCO_3^- and SO_4^{2-}/HCO_3^- molar ratios for the ground water samples. According to Han and Liu (in press), the rain water of the city of Guiyang is significantly enriched in Cl^-, NO_3^- and SO_4^{2-}. The average Cl^-/SO_4^{2-} molar ratio for Guiyang rain water is 0.36, within the range of the corresponding ratios for ground water studied here. Therefore, such ions in the surface and ground water can also be of atmospheric origin. However, SO_4^{2-} has complicated origins. As seen from Fig. 5, in addition to anthropogenic origins, SO_4^{2-} can be derived from the dissolution of gypsum and the oxidation of sulfide minerals. Three ground water samples collected from gypsum-containing and sulfide-containing aquifers show significantly high SO_4^{2-}/HCO_3^- but low Cl^-/HCO_3^- ratios, but show no clear influence on the water chemistry of other ground waters (Fig. 5). However, surface water samples collected in both winter and summer show significant contributions from both municipal sewage and dissolution of gypsum or oxidation of sulfide minerals in the aquifers (see inset diagram in Fig. 5).

The sewage samples have high Na^+ and K^+ concentrations during both seasons (Fig. 6), and they show better correlations with Cl^-. The incorporation of industrial and ubiquitously used NaCl, and potash fertilizers used in agricultural production into aquifers will lead to the increase of K^+ and Na^+ in ground and surface water in winter. As is shown in Fig. 6, the sewage samples have a relatively low K^+/Na^+ ratio, or are strongly enriched in Na^+ over K^+. The relationship between K^+/HCO_3^- and Na^+/HCO_3^- in surface and ground water in winter indicates that both surface and

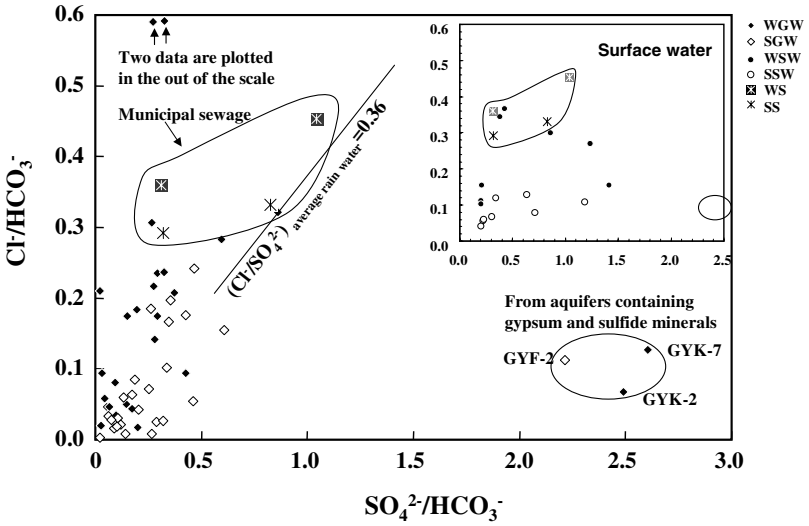

Fig. 5. Co-variations of HCO_3^- normalized SO_4^{2-} and Cl^- values (molar ratios) of ground water and surface water (inner figure) in Guiyang. The average Cl^-/SO_4^{2-} molar ratio of the rain water samples collected at Guiyang, from Han and Liu (in press), is also shown.

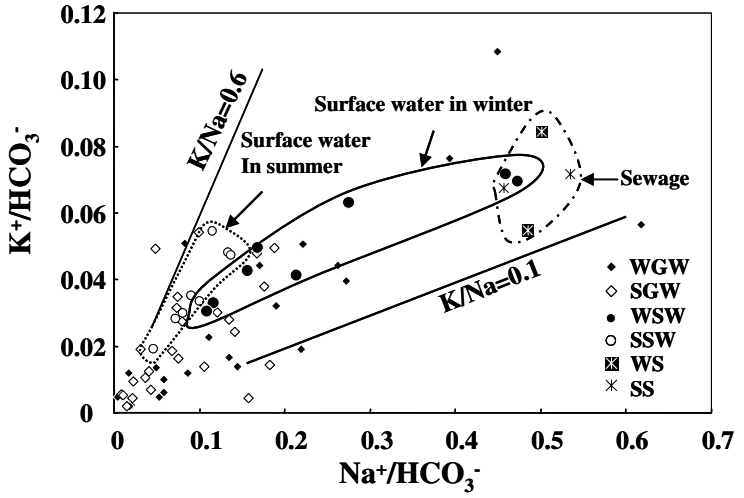

Fig. 6. Correlations of HCO_3^- normalized Na^+ and K^+ values (molar ratios) of the surface and ground waters of Guiyang.

ground water have received significant anthropogenic inputs. Unlike the surface water in winter, the surface water in summer has relatively high K^+/Na^+ and low Na^+/HCO_3^- ratios, showing a different mixing trend, or different sources of Na^+ and K^+ from that of the winter surface water.

The anthropogenic origin for most of K^+ and Na^+ in the studied water samples can be further demonstrated by the variations of Na^+/Sr^{2+} and K^+/Sr^{2+} with $^{87}Sr/^{86}Sr$ (Fig. 7). If Na^+ and K^+ are derived from weathering of silicate minerals, general positive correlations between $^{87}Sr/^{86}Sr$ and Na^+/Sr^{2+} and K^+/Sr^{2+} ratios should exist. However, except for some ground and summer surface water samples, most ground water and surface water in winter show big variations in Na^+/Sr^{2+} and K^+/Sr^{2+} ratios but with $^{87}Sr/^{86}Sr$ constant, suggesting anthropogenic sources of Na^+ and K+ in the water. The rain water samples studied by Han and Liu (in press) also have considerable variations of Na^+/Sr^{2+} and K^+/Sr^{2+} but constant Sr isotope ratios, the range and average values of which are also shown in Fig. 5. Since the rain waters collected over a year show large variability and significantly

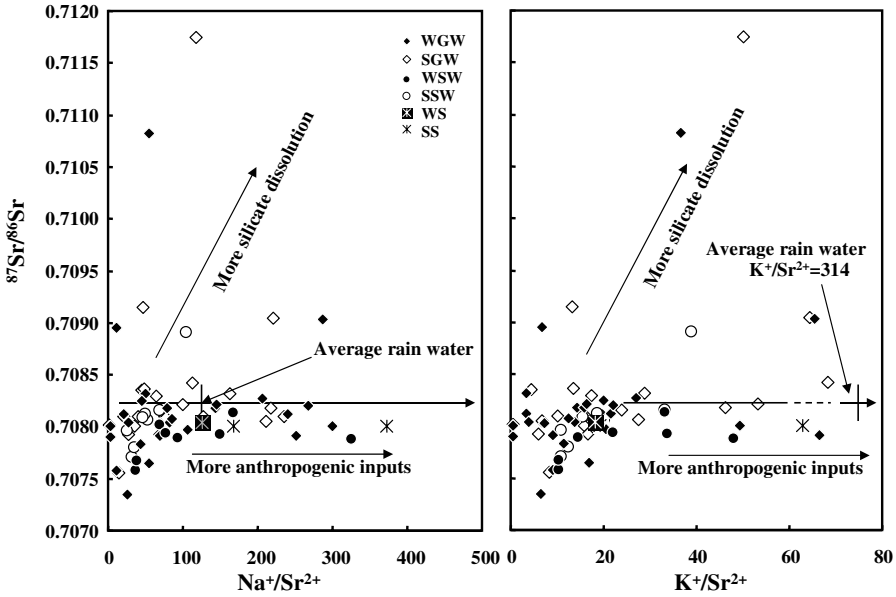

Fig. 7. Variation of $^{87}Sr/^{86}Sr$ with Na^+/Sr^{2+} and K^+/Sr^{2+} molar ratios of the ground and surface water of Guiyang. Also shown are the ranges of $^{87}Sr/^{86}Sr$ with Na^+/Sr^{2+} and K^+/Sr^{2+} molar ratios and their average values in rain waters of Guiyang city (Han and Liu, in press).

higher K^+/Sr^{2+} ratios, atmospheric input of K^+ into the surface and ground water is probably significant.

5.3. Control of water/rock interaction on solute source: constraints from Sr isotope data

Within the region studied, the aquifers are dominated by carbonate rocks (limestone and dolomite), followed by clastic sedimentary rocks, with gypsum and coal-bearing strata occurring locally. Dissolution of carbonate minerals and gypsum layers may, therefore, largely determine the chemical composition of water. The water samples collected at sampling site No. 2 have the highest TDS due to the existence of gypsum in the aquifer. Since Mg^{2+} and Ca^{2+} are not dominant contaminants, from the chemistry of the sewage samples, Sr isotope ratios ($^{87}Sr/^{86}Sr$) are plotted against Mg^{2+}/Ca^{2+} molar ratios for the water samples in order to assess the mineral-dissolution sources (Fig. 8). In the figure, except for the water samples GYK-32 and GYF-32 collected from a clastic-rock aquifer, which show the highest $^{87}Sr/^{86}Sr$ ratios, most of the data show relatively low $^{87}Sr/^{86}Sr$ ratios, distributed along a general mixing line between limestone and dolomite end-members. This confirms that weathering of carbonate rocks (limestone and dolomite) is the main source of the solutes in both ground and surface waters.

5.4. Carbonate mineral dissolution by soil CO_2: constraints from C isotope data

Fig. 9 shows a general decrease of C isotope values of DIC ($\delta^{13}C_{DIC}$) with increasing SO_4^{2-}/HCO_3^- ratios. Two ground water samples from a gypsum layer-containing aquifer deviate greatly from the main distribution trend of most water samples, showing the highest $\delta^{13}C_{DIC}$ values and SO_4^{2-}/HCO_3^- ratios. Sample GYK-7 is derived from oxidation of sulfide minerals and possibly organic S, characterized by a clearly high SO_4^{2-}/HCO_3^- ratio but a low $\delta^{13}C_{DIC}$ value. The municipal sewage samples in Fig. 9 deviate somewhat from the ground water distribution trend. Ground water sample GYK-15 shows the lowest $\delta^{13}C_{DIC}$ value, probably due to contamination by an oil leakage.

The geography of Guizhou Province is dominated by karst landforms, most soil CO_2 has $\delta^{13}C$ values from $-24‰$ to $-18.5‰$ (Zhou et al., 2002; Zheng, 1999), and hence the infiltrating water equilibrated with soil CO_2 (under open system conditions) will have $\delta^{13}C_{DIC}$ values of about $-16‰$ to $-10‰$, according to the estimation based on an equilibrium fractionation factor of $\sim+8‰$ between

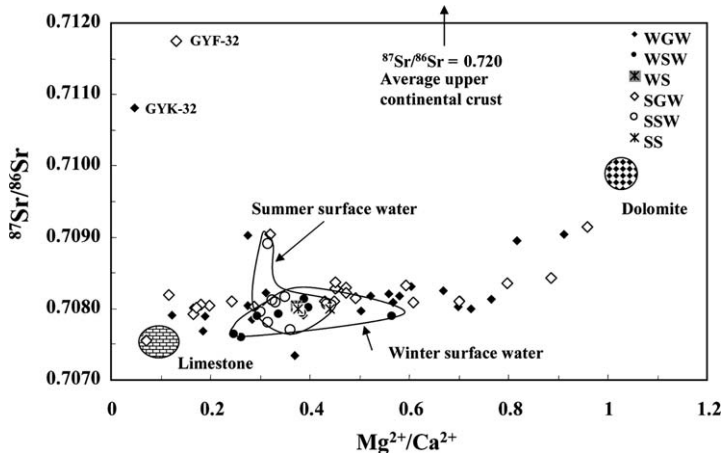

Fig. 8. Variations of $^{87}Sr/^{86}Sr$ ratios with Ca^{2+}/Mg^{2+} molar ratios of the surface and ground waters of Guiyang. The values of limestone and dolomite end-members are from Han and Liu (2004).

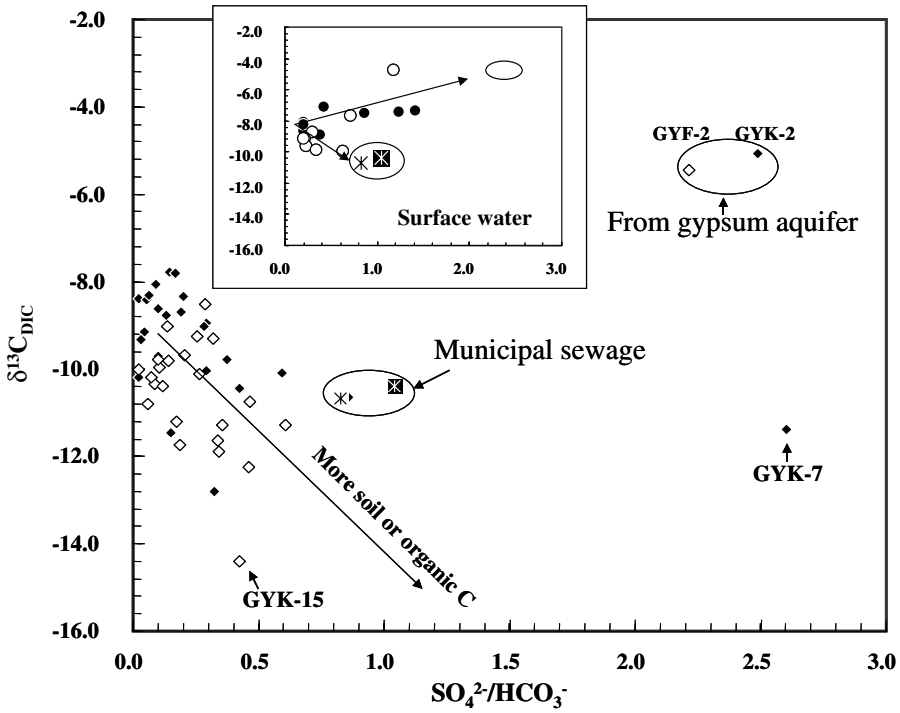

Fig. 9. Variations of $\delta^{13}C_{DIC}$ values with SO_4^{2-}/HCO_3^- molar ratios in the ground and surface water (inner diagram) of Guiyang.

soil CO_2 gas and dissolved HCO_3^- by Mook et al. (1974). In the case of congruent dissolution under a closed system condition, for every 2 moles of HCO_3^- added, one is derived from the carbonate rock, and one from soil CO_2. Nan et al. (1998) reported that Permian and Triassic limestone and dolomite, which are the most widely distributed strata in the studied area, have $\delta^{13}C_{DIC}$ values ranging from −1.8‰ to 4.8‰, averaging +2.5‰. Accordingly, the $\delta^{13}C_{DIC}$ values of the ground water dominated by calcite dissolution would be around −5‰ assuming an average $\delta^{13}C_{DIC}$ value of 2.5‰ for carbonate minerals. If the incongruent dissolution and congruent precipitation of carbonates under closed system conditions controlled the water chemistry, the $\delta^{13}C_{DIC}$ values of ground waters would increase and reach a value larger than −5‰. In general, the winter surface and ground

waters show higher $\delta^{13}C_{DIC}$ values (around −8.5‰), indicating that more inorganic C was derived from dissolution of marine carbonate minerals compared with the surface and ground waters in summer. On the other hand, most ground water in summer shows $\delta^{13}C_{DIC}$ values lower than −9‰, suggesting that soil C dissolution largely contributes to the DIC of most ground water, or that most ground water was in equilibration with, or open to, soil CO_2 in summer.

5.5. Carbonate dissolution by sulfuric acid

In addition to H_2CO_3, H_2SO_4 can also attack minerals, a fact observed by many authors (e.g. Hanshaw and Back, 1979; Macpherson, 1996; Montoroi et al., 2002; Massmann et al., 2003). The study by Han and Liu (2004) on water chemistry of the Wujiang River has also indicated that H_2SO_4 is involved in the erosion of the drainage basin. Fig. 10 shows the variations of the $[Ca^{2+} + Mg^{2+}]/[HCO_3^-]$ with $[SO_4^{2-}]/[HCO_3^-]$ equivalent ratios for the water samples. The chemical reactions that are most likely responsible for the chemistry of the waters studied here are also shown in the figure. According to the stoichiometric relationships of these chemical reactions, the mineral dissolution that occurred to control the chemistry of the waters can be inferred based on the variation in chemical composition shown in Fig. 10. For those waters that have $[Ca^{2+} + Mg^{2+}]/[HCO_3^-]$ ratios around unity and low $[SO_4^{2-}]/[HCO_3^-]$ ratios, carbonate mineral dissolution by H_2CO_3 dominates the mineral/water interaction. With increasing $[SO_4^{2-}]/[HCO_3^-]$ equivalent ratios, the $[Ca^{2+}+Mg^{2+}]/[HCO_3^-]$ ratio also increases, and more SO_4^{2-} is needed to balance the Ca^{2+} and the Mg^{2+} in the water samples. When carbonate mineral dissolution by both H_2CO_3 and H_2SO_4 takes place and reaches equilibrium, water should have a $[SO_4^2]/[HCO_3-]$ equivalent ratio of 0.5 and a $[Ca^{2+} + Mg^{2+}]/[HCO_3^-]$ ratio of 1.5, as shown by the cross point A in Fig. 10. When both $[SO_4^{2-}]/[HCO_3^-]$ and $[Ca^{2+} + Mg^{2+}]/[HCO_3^-]$ ratios continue to increase, dissolution of gypsum is needed to balance the negative and positive ions and so dominates water chemistry.

The co-variation of $[Ca^{2+} + Mg^{2+}]/[HCO_3^-]$ with $[SO_4^{2-}]/[HCO_3^-]$ ratios in Fig. 10 can also be interpreted in terms of binary mixing of HCO_3-type and SO_4-type water, that is, mixing of two end-members originating, respectively, from dissolution of carbonate minerals by H_2CO_3 and dissolution of gypsum. However, the correlation between $\delta^{13}C_{DIC}$ and SO_4^{2-}/HCO_3^- ratios in Fig. 9 does not support this interpretation, because the ground water from the gypsum layer-containing aquifer shows both high SO_4^{2-}/HCO_3^- ratios and $\delta^{13}C_{DIC}$ values. Therefore, mineral dissolution by H_2SO_4 is required to interpret the chemical composition of the water samples. Sulfuric acid in soil water can be formed from oxidation of sulfide minerals that are widely distributed in

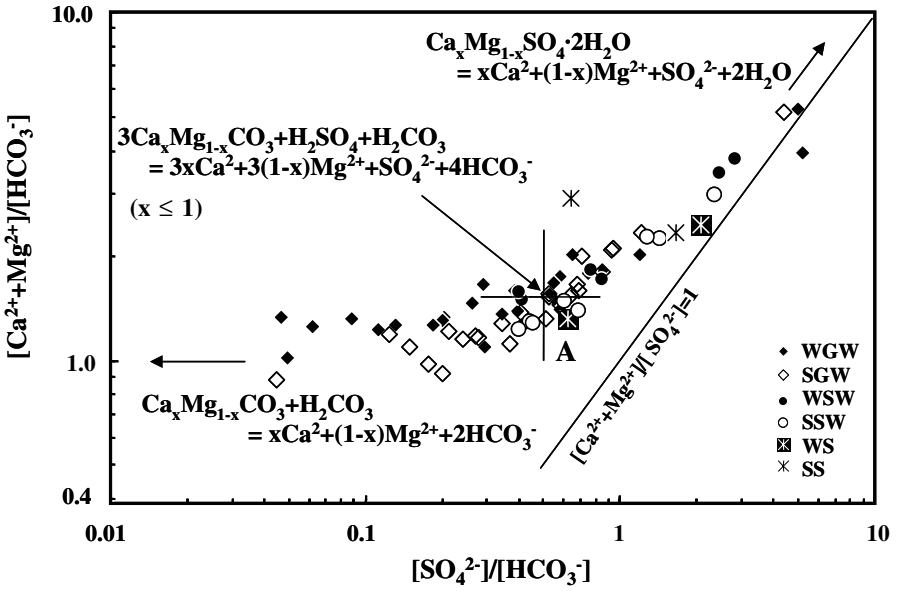

Fig. 10. Variations of $[Ca^{2+} + Mg^{2+}]/[HCO_3^-]$ with $[SO_4^{2-}]/[HCO_3^-]$ equivalent ratios of the surface and ground water of Guiyang.

coal-containing strata, and probably also from oxidation of organic S. The oxidation of sulfide minerals to form deposits of Fe hydroxide and a resulting increase in the H^+ content of the water is well demonstrated by the chemical features of sample GYK-7. In addition, acid rain events often occur in the city of Guiyang and are characterized by high contents of H_2SO_4 (Han and Liu, in press), and this probably is also an important source of H_2SO_4.

5.6. The roles of gypsum dissolution and sulfide oxidation

As described in the previous sections of this paper, the ground water from the gypsum-containing aquifer has the highest $\delta^{13}C_{DIC}$ values of around $-5‰$ and low $^{87}Sr/^{86}Sr$ ratios (Fig. 9), which might have resulted from the incongruent dissolution and congruent precipitation of carbonate minerals. The waters with the lowest ratios of SO_4^{2-}/HCO_3^- and $\delta^{13}C_{DIC}$ values of around $-10‰$ and $-8.5‰$ in summer and winter, respectively, could represent those waters whose chemical composition is controlled by carbonate dissolution mainly by H_2CO_3. In contrast, the waters with both high $\delta^{13}C_{DIC}$ and SO_4^{2-}/HCO_3^- ratios reflect the dissolution of carbonate minerals by H_2SO_4 or by alkaline water with high concentrations of HCO_3^-, which will result in high concentrations of SO_4^{2-} and of HCO_3^- from carbonate minerals, and hence in an increase of the $\delta^{13}C_{DIC}$ values.

Gypsum dissolution by H_2CO_3 or alkaline water will cause calcite precipitation due to the much higher solubility of gypsum than calcite as described in the following reaction:

$$HCO_3^- + CaSO_4 \cdot 2H_2O = CaCO_3 + SO_4^{2-} + H^+ + 2H_2O \quad (3)$$

The protons produced in the reaction will soon react with carbonate minerals in country rock, to increase the $\delta^{13}C_{DIC}$ values in ground waters: soil C depleted in ^{13}C will be first precipitated as calcite and more inorganic C as HCO_3^- released from carbonate mineral dissolution. Sample GYF-15 collected from a spring contaminated by oil leakage shows the lowest $\delta^{13}C_{DIC}$ value and a relatively high SO_4^{2-}/HCO_3^- ratio, suggesting that oxidation of organic matter by SO_4^{2-} in the ground water system may be responsible for the low $\delta^{13}C_{DIC}$ value and high SO_4^{2-} content of the water. The water GYK-7 plots far from the data distribution trend of most water samples, showing the highest SO_4^{2-}/HCO_3^- ratio due to oxidation of sulfide minerals in the aquifer. Its relatively low $\delta^{13}C_{DIC}$ value argues against an origin of carbonate mineral dissolution for DIC in the water.

6. Summary

The chemical compositions of the karst surface and ground water in both winter and summer are dominated by Ca^{2+}, Mg^{2+}, HCO_3^- and SO_4^{2-}, which account for more than 80% of the total cations and anions. During the summer, ground water has higher contents of most chemical components in comparison to surface water, due to dilution of surface water. Based on Sr isotope and chemical compositions, the studied karst surface and ground water samples have solutes mainly derived from dissolution of limestone and dolomite, with solutes resulting from dissolution of silicate minerals being very minor. The dissolution of sulfate evaporites (e.g. gypsum) and oxidation of sulfide minerals and organic S are the main factors leading to the increase of SO_4^{2-} in the water.

Anthropogenic inputs into the surface and ground water mainly include Na^+, K^+, Cl^-, NO_3^- and SO_4^{2-}, according to chemical compositions of municipal sewage and rain water in the city of Guiyang. In spatial variation, the ground water samples collected in the metropolitan area have higher Na^+, Cl^- and NO_3^- contents. In particular, Na^+ and Cl^- are higher in both surface and ground water in winter than in summer, demonstrating that both surface and ground water are susceptible to contamination resulting from low flow in the winter season. However, identification of specific sources for these anthropogenic components is difficult at the present stage. More isotope tracers are needed to trace the sources of different contaminants in the water.

The variations in chemical composition of both surface and ground water during different seasons demonstrate an active interaction or mass exchange between surface and ground water in karst environments, and indicate that the karst ground water system is vulnerable to impact by human activities. In both summer and winter, the ground waters have higher NO_3^- contents than surface water, indicating that conditions in the karstic ground water system do not favor denitrification, and hence is not easily self-remediated once contaminated by nitrates.

From the variations in chemical, and C and Sr isotopic composition, dissolution/precipitation of carbonate minerals are the important processes

controlling the water geochemistry of both surface and ground water in the karst area. Soil CO_2 dissolution largely contributes to the dissolved inorganic C of most ground water; in other words, shallow ground waters in particular were in equilibrium with, or open to soil CO_2. In addition, H_2SO_4, possibly produced as a result of oxidation of sulfides in S-rich coal seams and of organic S in soil as well as acid rain, is inferred to be involved in the dissolution of rocks and minerals. Dissolution of gypsum by H_2CO_3 may drive dissolution of carbonate minerals in the karst region studied.

Acknowledgements

This work was funded jointly by the Important Orientation Projects of the Chinese Academy of Sciences (KZCX3-SW-140, KZXCX2-105) and the National Natural Science Foundation of China (40273010). We thank the two anonymous reviewers for their constructive comments that have largely improved the scientific writing of this paper. Thanks are also due to Prof. Deming Mo of the Analysis Center of the Institute of Geochemistry, Chinese Academy of Sciences for his help and instruction during sample analyses.

References

Agrawal, G.D., Lunkad, S.K., Malkhed, T., 1999. Diffuse agricultural nitrate pollution of groundwaters in India. Water Sci. Technol. 39, 67–75.

Andreo, B., Carrasco, F., 1999. Application of geochemistry and radioactivity in the hydrogeological investigation of carbonate aquifers (Sierras Balance and Mijas, southern Spain). Appl. Geochem. 14, 283–299.

Barnes, C.J., Jacobason, G., Smith, G.D., 1992. The origin of high-nitrate waters in the Australian arid zone. J. Hydrol. 137, 181–197.

Desmarais, K., Rofstaczer, S., 2002. Inferring source waters from measurements of carbonate spring response to storms. J. Hydrol. 260, 118–134.

Gonfiantini, R., Zuppi, G.M., 2003. Carbon isotope exchange rate of DIC in karst ground water. Chem. Geol. 197, 319–336.

Han, Z.J., Jin, Z.S., 1996. Hydrology of Guizhou Province. Seismology Press, Beijing, p. 508 (in Chinese).

Han, G.L., Liu, C.-Q., 2004. Water geochemistry controlled by carbonate dissolution: a study of the river waters draining karst-dominated terrain, Guizhou Province, China. Chem. Geol. 204, 1–21.

Han, G.L., Liu, C.-Q. Strontium isotope and major ion chemistry of the rainwaters from Guiyang, Guizhou Province, China: Human impact on atmospheric environment. Sci. Total Environ. (in press).

Hanshaw, B.B., Back, W., 1979. Major geochemical processes in the evolution of carbonate-aquifer systems. J. Hydrol. 43, 287–312.

Jeong, C.H., 2001. Effect of land use and urbanization on hydrochemistry and contamination of groundwater from Taejon area, Korea. J. Hydrol. 253, 194–210.

Lee, E.S., Krothe, N.C., 2001. A four-component mixing model for water in a karst terrain in south-central Indian, USA: using solute concentration and stable isotopes as tracers. Chem. Geol. 179, 129–143.

Li, S.-L., Liu, C.-Q., Tao, F.-X., Lang, Y.-C., Han, G.-L., 2005. $\delta^{13}C_{DIC}$ as a tracer to monitor pollution and ecological changes in ground water. Ground Water 43, 494–499.

Macpherson, G.L., 1996. Hydrogeology of thin limestones – the Konza Prairie LTER Site. J. Hydrol. 186, 191–228.

Marfia, A.M., Krishnamurthy, R.V., Atekwana, E.A., Panton, W.F., 2004. Isotopic and geochemical evolution of ground and surface waters in a karst dominated geological setting: a case study from Belize, Central America. Appl. Geochem. 19, 937–946.

Massmann, G., Tichomirowa, M., Merz, C., Pekdeger, A., 2003. Sulfide oxidation and sulfate reduction in a shallow ground water system (Oderbruch Aquifer, Germany). J. Hydrol. 278, 231–243.

Montoroi, J.P., Grünberger, O., Nasri, S., 2002. Groundwater geochemistry of a small reservoir catchment in Central Tunisia. Appl. Geochem. 17, 1047–1060.

Mook, W.G., Bommerson, J.C., Staverman, W.H., 1974. Carbon isotope fractionation between dissolved bicarbonate and gaseous carbon dioxide. Earth Planet. Sci. Lett. 22, 169–176.

Nan, J., Zhou, D., Ye, J., Wang, Z., 1998. Geochemical studies on Permian–Triassic paleoclimate and paleo-ocean environment in Guizhou Province, China. Acta Mineral. Sinica 18, 239–249 (in Chinese with English Abstract).

Plummer, L.N., Busenberg, E., McConnell, J.B., Drenkard, S., Schlosser, P., Michel, R.L., 1998. Flow of river water into a Karstic limestone aquifer. 1. Tracing the young fraction in groundwater mixtures in the Upper Floridan Aquifer near Valdosta. Georgia. Appl. Geochem. 13, 995–1015.

Savoie, D.L., Prospero, J.M., 1989. Comparison of oceanic and continental sources of non-sea-salt sulfate over the Pacific Ocean. Nature 339, 685–687.

Scanlon, B.R., Mace, R.E., Barrett, M.E., Smith, B., 2003. Can we simulate regional groundwater flow in a karst system using equivalent porous media models? Case study, Barton Springs Edwards aquifer, USA. J. Hydrol. 276, 137–158.

Vaute, L., Drogue, C., Garrelly, L., Ghelfenstein, M., 1997. Relations between the structure of storage and the transport of chemical compounds in karstic aquifers. J. Hydrol., 221–238.

White, W., 2002. Karst hydrology: recent developments and open questions. Eng. Geol. 65, 85–106.

Wicks, C.M., Engeln, J.F., 1997. Geochemical evolution of a karst stream in Devils Icebox Cave, Missouri, USA. J. Hydrol. 198, 30–41.

Xiao, H.Y., Liu, C.-Q., 2002. Sources of nitrogen and sulfur in wet deposition at Guiyang, southwest China. Atmos. Environ. 36, 5121–5130.

Zheng, L., 1999. Carbon isotopic composition of soil carbon in karst area. Sci. China (D) 29, 514–519.

Zhou, Y., Zhang, P., Pan, G., Xiong, Z., Ran, J., 2002. Carbon fluxes in the interfaces of soil–air–water of epikarst ecosystem in short time scale: an example of daily dynamics in autumn as monitored in Maolan karst park. Guizhou. Quatern. Sci. 22, 258–265 (in Chinese with English Abstract).